NATIONAL ADVISORY COMMITTEE FOR AERONAUTICS

REPORT 1262

THEORETICAL AND EXPERIMENTAL INVESTIGATION OF THE EFFECT OF TUNNEL WALLS ON THE FORCES ON AN OSCILLATING AIRFOIL IN TWO-DIMENSIONAL SUBSONIC COMPRESSIBLE FLOW

By HARRY L. RUNYAN, DONALD S. WOOLSTON,
and A. GERALD RAINEY

1956

For sale by the Superintendent of Documents, U. S. Government Printing Office, Washington 25, D. C. Yearly subscription, $10; foreign, $11.25;
single copy price varies according to size --------- Price 25 cents

REPORT 1262

THEORETICAL AND EXPERIMENTAL INVESTIGATION OF THE EFFECT OF TUNNEL WALLS ON THE FORCES ON AN OSCILLATING AIRFOIL IN TWO-DIMENSIONAL SUBSONIC COMPRESSIBLE FLOW

By HARRY L. RUNYAN, DONALD S. WOOLSTON,
and A. GERALD RAINEY

Langley Aeronautical Laboratory
Langley Field, Va.

National Advisory Committee for Aeronautics

Headquarters, 1512 H Street NW., Washington 25, D. C.

Created by act of Congress approved March 3, 1915, for the supervision and direction of the scientific study of the problems of flight (U. S. Code, title 50, sec. 151). Its membership was increased from 12 to 15 by act approved March 2, 1929, and to 17 by act approved May 25, 1948. The members are appointed by the President, and serve as such without compensation.

JEROME C. HUNSAKER, Sc. D., Massachusetts Institute of Technology, *Chairman*

LEONARD CARMICHAEL, PH. D., Secretary, Smithsonian Institution, *Vice Chairman*

JOSEPH P. ADAMS, LL.B., Vice Chairman, Civil Aeronautics Board.

ALLEN V. ASTIN PH. D. Director. National Bureau of Standards.

PRESTON R. BASSETT, M. A., President, Sperry Gyroscope Co., Inc.

DETLEV W. BRONK, PH. D., President, Rockefeller Institute for Medical Research.

THOMAS S. COMBS, Vice Admiral, United States Navy, Deputy Chief of Naval Operations (Air).

FREDERICK C. CRAWFORD, Sc. D., Chairman of the Board, Thompson Products, Inc.

JAMES H. DOOLITTLE, Sc. D., Vice President, Shell Oil Co.

CLIFFORD C. FURNAS, PH. D., Assistant Secretary of Defense (Research and Development) Department of Defense.

CARL J. PFINGSTAG, Rear Admiral, United States Navy, Assistant Chief for Field Activities, Bureau of Aeronautics.

DONALD L. PUTT, Lieutenant General, United States Air Force, Deputy Chief of Staff (Development).

ARTHUR E. RAYMOND, Sc. D., Vice President—Engineering, Douglas Aircraft Co., Inc.

FRANCIS W. REICHELDERFER, Sc. D., Chief, United States Weather Bureau.

EDWARD V. RICKENBACKER, Sc. D., Chairman of the Board, Eastern Air Lines, Inc.

LOUIS S. ROTHSCHILD, PH. B., Under Secretary of Commerce for Transportation.

NATHAN F. TWINING, General, United States Air Force, Chief of Staff.

HUGH L. DRYDEN, PH. D., *Director*

JOHN W. CROWLEY, JR., B. S., *Associate Director for Research*

JOHN F. VICTORY, LL. D., *Executive Secretary*

EDWARD H. CHAMBERLIN, *Executive Officer*

HENRY J. E. REID, D. Eng., Director, Langley Aeronautical Laboratory, Langley Field, Va.

SMITH J. DEFRANCE, D. Eng., Director, Ames Aeronautical Laboratory, Moffett Field, Calif.

EDWARD R. SHARP, Sc. D., Director, Lewis Flight Propulsion Laboratory, Cleveland Airport, Cleveland, Ohio

---

LANGLEY AERONAUTICAL LABORATORY
Langley Field, Va.

AMES AERONAUTICAL LABORATORY
Moffett Field, Calif.

LEWIS FLIGHT PROPULSION LABORATORY
Cleveland Airport, Cleveland, Ohio

Conduct, under unified control, for all agencies, of scientific research on the fundamental problems of flight

REPORT 1262

THEORETICAL AND EXPERIMENTAL INVESTIGATION OF THE EFFECT OF TUNNEL WALLS ON THE FORCES ON AN OSCILLATING AIRFOIL IN TWO-DIMENSIONAL SUBSONIC COMPRESSIBLE FLOW [1]

By Harry L. Runyan, Donald S. Woolston, and A. Gerald Rainey

SUMMARY

This report presents a theoretical and experimental investigation of the effect of wind-tunnel walls on the air forces on an oscillating wing in two-dimensional subsonic compressible flow. A method of solving an integral equation which relates the downwash on a wing to the unknown loading is given, and some comparisons are made between the theoretical results and the experimental results. A resonance condition, which was predicted by theory in a previous report (NACA Rep. 1150), is shown experimentally to exist. In addition, application of the analysis is made to a number of examples in order to illustrate the influence of walls due to variations in frequency of oscillation, Mach number, and ratio of tunnel height to wing semichord.

INTRODUCTION

In the evaluation of results obtained by measurement of the forces on a wing in a wind tunnel, the question of the effect of the tunnel walls arises. In the case of steady flow the problem has been extensively investigated and, in general, relatively simple factors have been determined which can be used to modify measurements of the forces on a wing in a tunnel to correspond to free-air conditions. However, the corresponding problem of the effect of walls on an oscillating airfoil has received relatively little attention, particularly in the case of compressible flow. The present report concerns the wall effects in the oscillating case and treats the problem in two-dimensional subsonic compressible flow.

In incompressible flow, theoretical treatments of wall effects on oscillating wings have been made by several investigators and reported in references 1, 2, and 3. These investigators have shown generally that the tunnel-wall effects are a maximum for some small values of the reduced frequency and that the wall effects become negligible as the reduced frequency is increased. Extension of the theoretical treatment of the problem to include the effects of compressibility of the fluid has been reported in reference 4. In this reference, it is shown that, in addition to the large effect noted at low values of the reduced frequency, under certain conditions, large effects of the walls may be encountered at higher values of the reduced frequency. These effects are due to an acoustic resonant phenomenon which occurs when a disturbance from the oscillating wing is reflected from the tunnel wall back to the wing with such a phase relationship that it reinforces a succeeding disturbance.

In reference 4, the problem was expressed as an integral equation which relates the known downwash distribution over the airfoil to the unknown lift distribution. One purpose of the present report is to discuss further the integral equation and to demonstrate a method of solving it. A second purpose is to present some results showing wall effects calculated by this procedure and, in some cases, to compare the calculated results with experimental results. This phase of the investigation is given in three parts: (1) A comparison between analytically and experimentally determined values for the lift and moment on a wing oscillating in pitch at several subsonic Mach numbers; (2) an analytical study of the effects of a variation in Mach number for a constant ratio of tunnel height to wing semichord; and (3) an analytical study of the effects of a variation in the ratio of tunnel height to wing semichord. Portions of this material have been reported previously in reference 5 and are included in the present report in order to provide a more extensive and unified presentation.

As a check, the integral equation for the downwash on a wing oscillating between walls in a compressible medium is reduced to the zero-frequency condition and is given in the appendix. The resulting expression is in agreement with steady-state results.

The calculation procedure and the results contained in this report are of significance for such problems as the experimental measurement of the forces on an oscillating airfoil, the determination of wing-flutter characteristics in wind tunnels, and also in certain possible types of flutter of airfoils in cascade.

[1] Supersedes NACA Technical Note 3416 by Harry L. Runyan, Donald S. Woolston, and A. Gerald Rainey, 1955.

SYMBOLS

a	velocity of sound, ft/sec
A_n	coefficients in series expression for lift distribution (eq. (16)), where $n=0, 1, 2, \ldots$
b	wing semichord, ft
h	displacement of wing in vertical translation, ft
$\overline{H}$	height of tunnel, ft
H	height of tunnel referred to wing semichord
$H_0^{(2)}, H_1^{(2)}$	Hankel functions of the second kind
k	reduced-frequency parameter, $b\omega/U$
$\boldsymbol{K}(M,z)+\boldsymbol{K}(M,z,H)$	kernel of integral equation
$L(x_0), L(\theta_0)$	lift distribution, lb/ft/unit span
L_α	aerodynamic lift force per unit span due to pitch
L_h	aerodynamic lift force per unit span due to translation
M_α	aerodynamic moment per unit span due to pitch
M_h	aerodynamic moment per unit span due to translation
M	Mach number, U/a
$p=\frac{MkH}{2\pi\beta}$	
$R_n=\sqrt{(x-x_0)^2+\beta^2(nH)^2}$,	where $n=1,2,3, \ldots$
U	stream velocity in chordwise direction, ft/sec
$w(x)$	vertical induced velocity (perpendicular to chord), ft/sec
x_a	axis of rotation measured from midchord, positive rearward, based on semichord
x, x_0, y, ξ	Cartesian coordinates
$z=k(x-x_0)$	
α	angular displacement of wing in pitch, radians
$\beta=\sqrt{1-M^2}$	
$\epsilon=\frac{\lvert x-x_0\rvert}{\beta H}$	
$\theta=-\cos^{-1}x$	
$\theta_0=-\cos^{-1}x_0$	
$\mu=\frac{Mk}{\beta^2}$	
ρ	fluid density, slugs/cu ft
ϕ_{L_α}	phase angle between lift force and position of pitching wing, deg
ϕ_{L_h}	phase angle between lift force and position of translating wing, deg
ϕ_{M_α}	phase angle between moment and position of pitching wing, deg
ϕ_{M_h}	phase angle between moment and position of translating wing, deg
ω	circular frequency of oscillation, radians/sec
ω_{res}	circular frequency at resonance, radians/sec
Δp	pressure difference between upper and lower surface, lb/sq ft

Primed quantities refer to a wing in free air.

ANALYTICAL INVESTIGATION

This section is concerned with the development of a method for solving the integral equation, originally derived in reference 4, which relates the downwash to the loading on an oscillating wing. The basic integral equation and its kernel is given by equations (1) and (2). Reduction of the kernel is made in equations (3) to (10). Alternative series expressions for the kernel which are suitable for numerical computation are given by equations (11) to (15). The loading on the wing is given by equation (16), the downwash expression by equations (18) and (19), and finally the lift and moment expressions by equations (20).

THE INTEGRAL EQUATION AND ITS KERNEL FUNCTION

The integral equation.—The integral equation of reference 4 for the vertical velocity or downwash of an oscillating airfoil between plane walls may be written as

$$w(x)=\frac{\omega b}{\rho U^2}\int_{-1}^{1} L(x_0)[\boldsymbol{K}(M,z)+\boldsymbol{K}(M,z,H)]dx_0 \tag{1}$$

where $w(x)$ is the known vertical velocity (or known motion of the wing) and $L(x_0)$ is the unknown lift distribution or the local strength of a distribution of oscillating pressure doublets. The functions within the brackets comprise the kernel function of the integral equation and appear formally as

$$\boldsymbol{K}(M,z)=\frac{i}{4\beta k}\lim_{y\to 0} e^{-ik(x-x_0)}\int_{-\infty}^{x-x_0} e^{\frac{ik}{\beta^2}\xi}\frac{\partial^2}{\partial y^2}H_0^{(2)}\left(\frac{Mk}{\beta^2}\sqrt{\xi^2+\beta^2y^2}\right)d\xi \tag{2a}$$

$$\boldsymbol{K}(M,z,H)=\frac{i}{4\beta k}\lim_{y\to 0} e^{-ik(x-x_0)}\int_{-\infty}^{x-x_0} 2\sum_{n=1}^{\infty}(-1)^n e^{\frac{ik}{\beta^2}\xi}\frac{\partial^2}{\partial y^2}H_0^{(2)}\left[\frac{Mk}{\beta^2}\sqrt{\xi^2+\beta^2(y-nH)^2}\right]d\xi \tag{2b}$$

The first function $\boldsymbol{K}(M, z)$ corresponds to the kernel for the free-air condition as given by Possio (ref. 6). The second function $\boldsymbol{K}(M, z, H)$, containing the infinite summation, is the additional part of the kernel arising from the effect of the walls. Physically, a kernel function represents the contribution to the vertical velocity at a field point due to a pulsating pressure doublet of unit strength located at any other point in the field. For the particular case represented by equations (2), the kernel function gives the vertical velocity in the plane of a wing located in the center of the tunnel. The expression $\boldsymbol{K}(M, z)$ gives the downwash of a doublet in the plane of the wing, whereas the expression $\boldsymbol{K}(M, z, H)$ gives the downwash due to the system of images which mathematically represents the walls.

Reduction of the kernel function—The integrals contained in the expressions for the kernel function in equations (2) are improper because they have an infinite limit and also because, at certain points, the integrands become singular. This section is concerned with the reduction of these integrals to a form more amenable to computation.

By making use of the fact that the Hankel functions in equations (2) satisfy the identity

$$\frac{\partial^2}{\partial y^2} H_0^{(2)}\left(\frac{Mk}{\beta^2}\sqrt{\xi^2+\beta^2y^2}\right)=-\beta^2\frac{\partial^2}{\partial\xi^2}H_0^{(2)}\left(\frac{Mk}{\beta^2}\sqrt{\xi^2+\beta^2y^2}\right)-\frac{M^2k^2}{\beta^2}H_0^{(2)}\left(\frac{Mk}{\beta^2}\sqrt{\xi^2+\beta^2y^2}\right) \tag{3}$$

there is obtained for the downwash

$$\begin{aligned} w(x)=&\frac{\omega b}{\rho U^2}\frac{-i}{4\beta k}\lim_{y\to 0}\int_{-1}^{1}L(x_0)e^{-ik(x-x_0)}\left(\beta^2\int_{-\infty}^{x-x_0}e^{\frac{ik}{\beta^2}\xi}\frac{\partial^2}{\partial\xi^2}H_0^{(2)}\left(\frac{Mk}{\beta^2}\sqrt{\xi^2+\beta^2y^2}\right)d\xi+\right.\\ &\frac{M^2k^2}{\beta^2}\int_{-\infty}^{x-x_0}e^{\frac{ik}{\beta^2}\xi}H_0^{(2)}\left(\frac{Mk}{\beta^2}\sqrt{\xi^2+\beta^2y^2}\right)d\xi+\\ &2\sum_{n=1}^{\infty}(-1)^n\left\{\beta^2\int_{-\infty}^{x-x_0}e^{\frac{ik}{\beta^2}\xi}\frac{\partial^2}{\partial\xi^2}H_0^{(2)}\left[\frac{Mk}{\beta^2}\sqrt{\xi^2+\beta^2(y-nH)^2}\right]d\xi+\right.\\ &\left.\left.\frac{M^2k^2}{\beta^2}\int_{-\infty}^{x-x_0}e^{\frac{ik}{\beta^2}\xi}H_0^{(2)}\left[\frac{Mk}{\beta^2}\sqrt{\xi^2+\beta^2(y-nH)^2}\right]d\xi\right\}\right)dx_0 \end{aligned} \tag{4}$$

The integrals of equation (4) that contain partial derivatives of Hankel functions can be integrated twice by parts to obtain

$$\begin{aligned} &\int_{-\infty}^{x-x_0}e^{\frac{ik}{\beta^2}\xi}\frac{\partial^2}{\partial\xi^2}H_0^{(2)}\left[\frac{Mk}{\beta^2}\sqrt{\xi^2+\beta^2(y-nH)^2}\right]d\xi\equiv-\frac{Mk}{\beta^2}e^{\frac{ik}{\beta^2}(x-x_0)}\frac{x-x_0}{\sqrt{(x-x_0)^2+\beta^2(y-nH)^2}}H_1^{(2)}\left[\frac{Mk}{\beta^2}\sqrt{(x-x_0)^2+\beta^2(y-nH)^2}\right]-\\ &\frac{ik}{\beta^2}e^{\frac{ik}{\beta^2}(x-x_0)}H_0^{(2)}\left[\frac{Mk}{\beta^2}\sqrt{(x-x_0)^2+\beta^2(y-nH)^2}\right]-\frac{k^2}{\beta^4}\int_{-\infty}^{x-x_0}e^{\frac{ik}{\beta^2}\xi}H_0^{(2)}\left[\frac{Mk}{\beta^2}\sqrt{\xi^2+\beta^2(y-nH)^2}\right]d\xi \end{aligned} \tag{5}$$

The last integral of equation (5) may be written in two parts as

$$\begin{aligned} &\sum_{n=1}^{\infty}(-1)^n\int_{-\infty}^{x-x_0}e^{\frac{ik}{\beta^2}\xi}H_0^{(2)}\left[\frac{Mk}{\beta^2}\sqrt{\xi^2+\beta^2(y-nH)^2}\right]d\xi\\ &=\int_0^{\infty}e^{-\frac{ik}{\beta^2}\xi}\sum_{n=1}^{\infty}(-1)^nH_0^{(2)}\left[\frac{Mk}{\beta^2}\sqrt{\xi^2+\beta^2(y-nH)^2}\right]d\xi+\\ &\int_0^{x-x_0}e^{\frac{ik}{\beta^2}\xi}\sum_{n=1}^{\infty}(-1)^nH_0^{(2)}\left[\frac{Mk}{\beta^2}\sqrt{\xi^2+\beta^2(y-nH)^2}\right]d\xi \end{aligned} \tag{6}$$

The first integral on the right-hand side of equation (6) will be left temporarily in integral form and will be treated in the following section. (See evaluation of S_3 following eq. (13).)

The second integral on the right-hand side of equation (6) has not been integrated in closed form; however, in wind-tunnel problems it can be handled conveniently by approximate methods. (An alternative means of treating this integral, which avoids the approximation but is somewhat more tedious, will be indicated in the discussion following eq. 14(c).) A practical assumption which is often made in the analysis of the effect of wind-tunnel walls is that the tunnel height is considered large compared with the wing semichord. With this assumption the argument of the Hankel function in equation (6) can be written as (in the limit as $y\to 0$)

$$\frac{Mk}{\beta^2}\sqrt{\xi^2+\beta^2(nH)^2}=\frac{Mk}{\beta^2}\beta nH\sqrt{\left(\frac{\xi}{\beta nH}\right)^2+1}\approx\frac{Mk}{\beta}nH$$

provided that $\frac{\xi}{\beta nH}\ll 1$.

This approximation implies that the airfoil images, and, particularly the closest image $n=1$, are a sufficient distance from the airfoil so that the actual distance $\sqrt{\xi^2+\beta^2(nH)^2}$ may be replaced by the vertical distance βnH of the image above the airfoil. Of course, this approximation does not hold for Mach numbers close to or equal to unity. With this approximation, the second integral of equation (6) can be expressed as

$$\begin{aligned} &\lim_{y\to 0}\int_0^{x-x_0}e^{\frac{ik}{\beta^2}\xi}\sum_{n=1}^{\infty}(-1)^nH_0^{(2)}\left[\frac{Mk}{\beta^2}\sqrt{\xi^2+\beta^2(y-nH)^2}\right]d\xi\\ &=\sum_{n=1}^{\infty}(-1)^nH_0^{(2)}\left(\frac{MknH}{\beta}\right)\int_0^{x-x_0}e^{\frac{ik}{\beta^2}\xi}d\xi\\ &=\sum_{n=1}^{\infty}(-1)^nH_0^{(2)}\left(\frac{MknH}{\beta}\right)\frac{\beta^2}{ik}\left[e^{\frac{ik}{\beta^2}(x-x_0)}-1\right] \end{aligned} \tag{7}$$

and these equations may be used to express equation (4) as

$$w(x)=\frac{\omega b}{\rho U^2}\int_{-1}^{1}L(x_0)[\boldsymbol{K}(M,z)+\boldsymbol{K}(M,z,H)]dx_0 \tag{8}$$

where

$$\begin{aligned} \boldsymbol{K}(M,z)=&\frac{1}{4\beta}e^{-iz}\left\{e^{\frac{iz}{\beta^2}}\left[-H_0^{(2)}(\mu R_0)+\frac{iM(x-x_0)}{|x-x_0|}H_1^{(2)}(\mu R_0)\right]+\right.\\ &\left.i\beta^2\left[\frac{2}{\pi\beta}\log_e\frac{1+\beta}{M}+\int_0^{\frac{v}{M}}e^{iu}H_0^{(2)}(M|u|)du\right]\right\} \end{aligned} \tag{9}$$

and

$$\begin{aligned} \boldsymbol{K}(M,z,H)=&\frac{e^{-iz}}{2\beta}\left[-e^{\frac{iz}{\beta^2}}\sum_{n=1}^{\infty}(-1)^nH_0^{(2)}(\mu R_n)+\right.\\ &\beta^2\left(e^{\frac{iz}{\beta^2}}-1\right)\sum_{n=1}^{\infty}(-1)^nH_0^{(2)}\left(\frac{MknH}{\beta}\right)+\\ &ik\sum_{n=1}^{\infty}(-1)^n\int_0^{\infty}e^{-\frac{ik}{\beta^2}\xi}H_0^{(2)}\left[\frac{kM}{\beta^2}\sqrt{\xi^2+\beta^2(nH)^2}\right]d\xi+\\ &\left.e^{\frac{iz}{\beta^2}}\sum_{n=1}^{\infty}(-1)^n\frac{iM(x-x_0)}{R_n}H_1^{(2)}(\mu R_n)\right] \end{aligned} \tag{10}$$

in which use has been made of

$$\mu=\frac{kM}{\beta^2} \qquad u=\frac{k}{\beta^2}\xi \qquad v=\frac{Mz}{\beta^2}$$

$$R_0=|x-x_0| \qquad R_n=\sqrt{(x-x_0)^2+\beta^2(nH)^2}$$

Equation (8), together with the definition of equations (9) and (10), permits the determination of the effect of tunnel walls on a lift distribution $L(\theta_0)$ for a given downwash distribution $w(x)$. The integral equation for the case of no tunnel walls checks the results of Possio (ref. 6). For the case with walls and for the limiting steady-flow case of zero frequency, it is possible to obtain a mathematical check with some existing results; this check is shown in the appendix.

Alternative series expressions for kernel.—Although the form of the kernel $\boldsymbol{K}(M,z,H)$, given by equation (10), could be used for calculation, alternative series which are more highly convergent may be used and are given in this section.

The kernel $\boldsymbol{K}(M,z,H)$ is the sum of four infinite series which can be written as

$$\boldsymbol{K}(M,z,H)=\frac{e^{-iz}}{2\beta}(C_1S_1+C_2S_2+C_3S_3+C_4S_4) \tag{11}$$

where the S_n's denote the indicated infinite summations of equation (10) and the C_n's the respective multipliers.

Series S_1 and S_2 of equation (11) may be put in a more rapidly convergent form according to Infeld, Smith, and Chien (ref. 7). When the variables p and ϵ are introduced, where

$$p=\frac{MkH}{2\pi\beta}$$

and

$$\epsilon=\frac{|x-x_0|}{\beta H}$$

the series S_1 and S_2 can be written as

$$\begin{aligned}S_1&=\sum_{n=1}^{\infty}(-1)^n H_0^{(2)}(\mu R_n)\\&=\sum_{n=1}^{\infty}(-1)^n H_0^{(2)}\left(2\pi p\sqrt{\epsilon^2+n^2}\right)\\&=\frac{1}{2\pi}\left[\frac{2ie^{-\pi\epsilon\sqrt{1-4p^2}}}{\sqrt{1-4p^2}}+2i\sum_{n=1}^{\infty}\frac{e^{-\pi\epsilon\sqrt{(2n+1)^2-4p^2}}}{\sqrt{(2n+1)^2-4p^2}}+\right.\\&\left.\frac{e^{-\pi\epsilon\sqrt{(2n-1)^2-4p^2}}}{\sqrt{(2n-1)^2-4p^2}}-\pi H_0^{(2)}(2\pi\epsilon p)\right]\end{aligned} \tag{12}$$

and

$$\begin{aligned}S_2&=\sum_{n=1}^{\infty}(-1)^n H_0^{(2)}\left(\frac{MknH}{\beta}\right)\\&=\sum_{n=1}^{\infty}(-1)^n H_0^{(2)}(2\pi np)\\&=\frac{1}{2\pi}\left\{-\pi+2i(\gamma+\log_e 2p)+4i\sum_{n=1}^{\infty}\left[\frac{1}{\sqrt{(2n-1)^2-4p^2}}-\frac{1}{2n-1}\right]\right\}\end{aligned} \tag{13}$$

where Euler's constant $\gamma=0.577215$.

Series S_3 may be evaluated by utilizing the expression for S_1 (eq. (12)) and integrating the resulting expression to obtain

$$S_3=\int_0^{\infty}e^{-\frac{ik}{\beta^2}\xi}\sum_{n=1}^{\infty}(-1)^n H_0^{(2)}\left[\frac{kM}{\beta^2}\sqrt{\xi^2+\beta^2(nH)^2}\right]d\xi \tag{14a}$$

$$\begin{aligned}S_3=&-\frac{1}{2}\int_0^{\infty}e^{-\frac{ik}{\beta^2}\xi}H_0^{(2)}\left(\frac{kM\xi}{\beta^2}\right)d\xi+\\&\frac{2i\beta}{M}\sum_{n=0}^{\infty}\frac{1}{\sqrt{(2n+1)^2\left(\frac{\pi\beta}{M}\right)^2-(kH)^2}}\times\\&\int_0^{\infty}e^{-\xi\left[\frac{ik}{\beta^2}+\frac{M}{\beta^2H}\sqrt{(2n+1)^2\left(\frac{\pi\beta}{M}\right)^2-(kH)^2}\right]}d\xi\end{aligned} \tag{14b}$$

$$\begin{aligned}S_3=&-\frac{\beta}{\pi k}\log_e\frac{1+\beta}{M}+\\&\frac{2i\beta}{M}\sum_{n=0}^{\infty}\frac{1}{\left(\frac{\pi}{\beta H}\right)^2[(2n+1)^2-4p^2]+\left(\frac{k}{\beta^2}\right)^2}\left[\frac{M}{\beta^2H}-\right.\\&\left.i\frac{k/\beta^2}{\frac{\pi\beta}{M}\sqrt{(2n+1)^2-4p^2}}\right]\end{aligned} \tag{14c}$$

It is of interest to note that series S_3 may be employed in an alternative means of integrating equation (7). For application to wind-tunnel problems, where the ratio of tunnel height to wing semichord is small, or in application to cascade problems, the approximation employed in integrating equation (7) becomes less valid. It is possible to avoid the use of the approximation by writing the integral of equation (7) in a form which is identical to that of equations (14a) and (14b) with the exception of the upper limit. The integral containing the Hankel function can be evaluated by employing the tables of Schwarz (ref. 8). The second integral, containing only an exponential term, can be integrated in closed form, as was done to obtain equation (14c).

Series S_4 may be evaluated in a direct manner by employing tables of the Hankel function and by using for large values of the argument the approximation

$$H_1^{(2)}(\mu R_n)\approx\sqrt{\frac{2}{\pi\mu R_n}}\,e^{-i\left(\mu R_n-\frac{3}{4}\pi\right)} \tag{15}$$

With the aid of series S_1, S_2, S_3, and S_4, the kernel $\boldsymbol{K}(M,z,H)$ may be evaluated.

METHOD OF SOLUTION

A method of using equation (8) to determine the aerodynamic forces on a wing oscillating in the presence of plane walls is now discussed. The method under consideration is one of collocation similar to that used by Possio (ref. 6) and Frazer (ref. 9) for the case of no walls. The approach involves the assumption of an appropriate series expression for the lift distribution, substitution of this series in the integral equation for the downwash, and calculation of the

downwash at arbitrarily selected points on the chord (control points). Thus equation (8) is reduced to a set of simultaneous equations, the unknowns of which are the coefficients of the assumed expression for the loading.

Expression for the loading.—The expression which is assumed for the lift distribution is a trigonometric series expansion which satisfies the Kutta condition at the trailing edge and which has the proper type of singularity at the leading edge. This expression is

$$\frac{L(x_0)}{\rho U^2}=A_0 \cot \frac{\theta_0}{2}+\sum_{n=1}^{\infty} A_n \sin n\theta_0=L(\theta_0) \tag{16}$$

where $x_0=-\cos\theta_0$ and the A_n's are unknown coefficients to be determined in accordance with the downwash $w(x)$, which is known from the motion of the wing. It is desirable to rewrite equation (8) in terms of the variable θ_0 as follows:

$$w(x)=Uk\left[\int_0^{\pi} L(\theta_0)\boldsymbol{K}(M,z)\sin\theta_0 d\theta_0+\int_0^{\pi} L(\theta_0)\boldsymbol{K}(M,z,H)\sin\theta_0 d\theta_0\right] \tag{17}$$

The first integral on the right-hand side of equation (17) is the integral expression first derived by Possio (ref. 6) for the condition of no walls. Its solution has been treated by several investigators (see, for example, ref. 9) and will not be discussed herein. It can be expressed entirely in terms of the unknown coefficients A_n of equation (16). The second integral of equation (17) may be evaluated by the use of equations (12), (13), (14), and (15).

Determination of the aerodynamic forces.—The integrals of equation (17) are determined for a selected number of control points and equated to the expression for the downwash. The expression relating the downwash to the motion of a wing translating (h) and pitching (α) about an axis located at x_a is

$$w(x)=\dot{h}+U\alpha+b(x-x_a)\dot{\alpha} \tag{18}$$

or, with the assumption of harmonic motion,

$$\frac{w(x)}{U}=ik\frac{h}{b}+[1+ik(x-x_a)]\alpha \tag{19}$$

Equation (19) is used to calculate $w(x)$ for values of x appropriate to each of the selected control points. A set of simultaneous equations can then be written, the number of which corresponds to the number of control points employed and (conveniently) to the number of terms retained in the series for $L(\theta_0)$. The unknown coefficients may now be determined by solving these simultaneous equations. The total lift and moment about the midchord are given in terms of the coefficients A_n through the relations

$$\left.\begin{aligned}\frac{-L_\alpha}{\pi\rho bU^2}&=\frac{1}{2}\left(A_0+\frac{1}{2}A_1\right)\\ \frac{M_\alpha}{\pi\rho b^2U^2}&=\frac{1}{8}\left(A_0+\frac{1}{2}A_2\right)\end{aligned}\right\} \tag{20}$$

Effect of the number of control points considered.—An investigation was made of the number of terms of the series for the lift distribution (eq. (16)) and thus of the number of control points required to obtain satisfactory accuracy. Calculations were performed for a particular case by increasing the number of control points and the number of terms of the loading series until the solutions were in reasonable agreement. For the case considered, three terms of the series for the lift and three control points at the quarter-, half-, and three-quarter-chord positions gave satisfactory results. The consideration of two additional control points at the leading and trailing edges, together with two additional terms of the lift series, made no significant change in the results. For high values of the reduced-frequency parameter k, the use of additional control points might be necessary.

The procedure just discussed involves consideration of a continuous distribution of pressure doublets over the chord. Calculations requiring much less computing can be made by considering the chordwise loading to be concentrated in a single doublet located at the quarter chord and by satisfying the downwash at the three-quarter chord. In the case of the lift, this approach has been found to give fairly good agreement with the results of the more elaborate calculations except in the vicinity of the resonant frequency.

THE ANALYTICALLY INDICATED RESONANCE PHENOMENON

Two-dimensional tunnel.—By examination of equations (12) and (13), it may be seen that the series S_1 and S_2 become infinite when

$$4p^2=(2n-1)^2$$

or where

$$\frac{\omega\overline{H}}{a}=\pi\beta(2n-1) \qquad (n=1,2,3,\ .\ .\ .) \tag{21}$$

At these critical values of the frequency parameter, the expression for the kernel $\boldsymbol{K}(M,z,H)$ (eq. (11)) becomes infinite for all values of x. Physically, this condition represents a resonance in the tunnel involving a transverse oscillation of the moving air between the walls.

The fundamental or smallest critical values of $\omega\overline{H}/a$ corresponding to $n=1$ in equation (21) are shown plotted as functions of Mach number M in figure 1. Equation (21) and figure 1 show that finite values of the critical frequency exist for the condition $M=0$, $U=0$, and $a\neq\infty$. These conditions correspond to a compressible fluid at zero velocity in the tunnel. As the Mach number is increased, the critical-frequency parameter decreases rapidly and becomes zero at a Mach number of unity.

As indicated by equation (1), the product of the lift and the kernel function must remain equal to the vertical velocity over the wing; this velocity is defined by the motion of the wing and remains finite. The product of the lift and the kernel function can remain finite only if the lift approaches zero as the kernel becomes infinite. This condition in the tunnel is analogous to the well-known case of a simple undamped-spring-mass system for which, at the resonant frequency, theory predicts an infinite deflection of the mass occurring even with a forcing function of small amplitude.

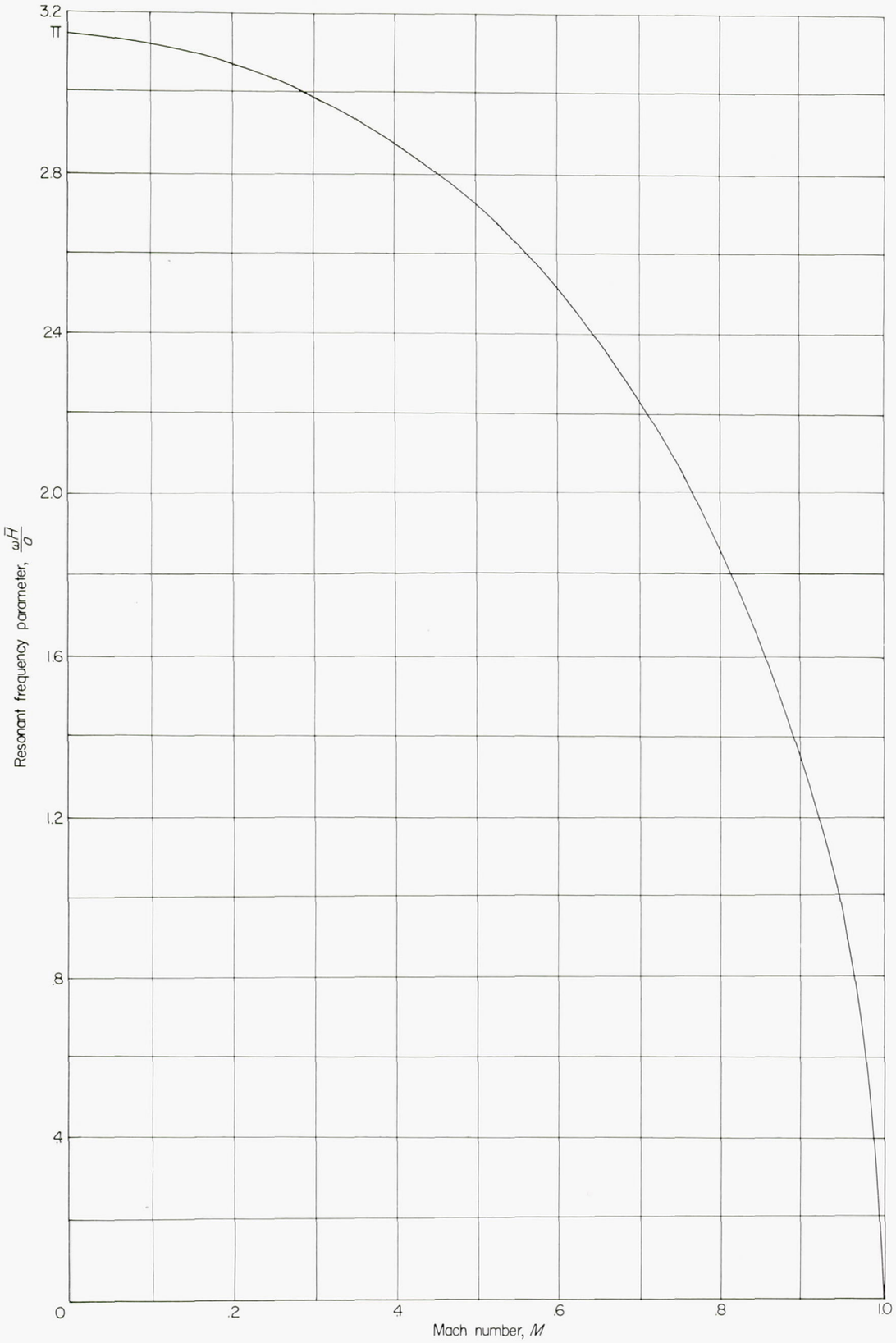

FIGURE 1.—Fundamental values of resonant frequency parameter $\frac{\omega \overline{H}}{a}$ as a function of Mach number.

Circular tunnel.—A resonance can also be demonstrated for the infinite circular tunnel. The nature of the boundary-value problem, for this case, makes it possible to separate variables; therefore, the governing partial-differential equation can be reduced to Bessel's equation. (See, for instance, ref. 10.) The resonant frequencies are then found as the roots of the equation

$$J_n'\left(\frac{\omega D}{2a\beta}\right)=0 \qquad (n=0, 1, 2, \ldots)$$

or

$$\frac{\omega D}{2a}=\rho_n\beta$$

where J_n represents the Bessel function of the first kind, D is the tunnel diameter, and ρ_n is the root of the equation

$$J_n'(\rho_n)=0$$

Values for ρ_n for the first several modes are $\rho_n=1.84$, 3.05, and 4.17. Note that, for a circular tunnel having a diameter equal to the height of a plane tunnel, the fundamental frequency is $3.68/\pi=1.17$ higher than resonant frequency in the plane tunnel discussed in this report.

EXPERIMENTAL INVESTIGATION

WIND TUNNEL

The experimental part of the investigation of the effect of tunnel walls on the forces acting on an oscillating airfoil was conducted in the Langley 2- by 4-foot flutter research tunnel. For these tests, a rectangular test section having dimensions of 2 feet by 3.8 feet was used. This tunnel is of the closed-throat, single-return type and employs either air or Freon-12 as a testing medium at pressures from 1 atmosphere down to about ⅛ atmosphere.

It has been shown previously that the resonant frequency varies directly as the speed of sound. Inasmuch as Freon-12 has a speed of sound equal to about one-half that of air, the experiments to be discussed were conducted in Freon-12 so that the resonant frequency could be surveyed within he frequency limitations of the equipment.

MODEL AND OSCILLATING MECHANISM

Figure 2 is a schematic drawing of the test section with the model and oscillating mechanism installed. The model had a chord of 1 foot and an NACA 65–010 airfoil section; it completely spanned the 2-foot dimension of the test section. The gaps between the model and the tunnel wall were sealed by end plates which rotated with the model. The model, driven symmetrically from both ends, was oscillated in pitch about the midchord by a direct-drive eccentric-cam system powered by an induction motor with variable frequency supply.

INSTRUMENTATION

The lift and moment on the wing were obtained by electrical integration of the outputs of 12 model 49–TP

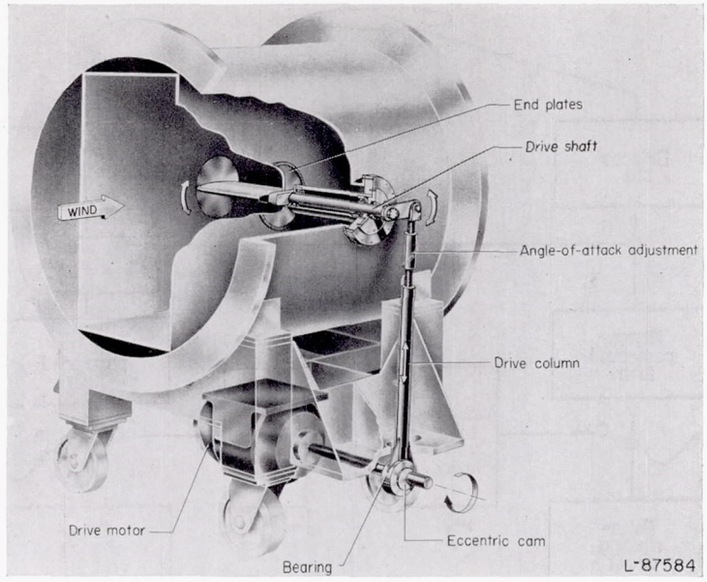

FIGURE 2.—Schematic drawing of test section with model and oscillating mechanism installed.

NACA miniature electrical pressure gages. The pressure gages, which are described in considerable detail in reference 11, were located at the center of the span at 2.5, 5, 10, 15, 20, 30, 40, 50, 60, 70, 80, and 90 percent of the chord. Each gage was arranged to indicate the difference in pressure between orifices on the upper and lower surfaces. Electrical integration techniques used in these experiments are discussed in reference 12. The so-called square-wave method of weighting was used; that is, the pressure indicated by each gage was assumed to represent the pressure acting over a portion of the chord extending one-half the distance to the next gage both forward and rearward. For example, the fraction of the chord assigned to the first gage was 3.75 percent and to the sixth gage was 10 percent. Some of the implications of this method of integration will be discussed in a subsequent section.

The angular displacement at the midspan position was indicated by resistance-wire strain gages attached to a torque rod running through the center of the hollow wing. One end of the torque rod was fixed to the center of the wing and the other end was fixed to the tunnel wall.

A schematic diagram of the instrumentation is shown in figure 3. The magnitude of the vector representing the fundamental component of lift or moment and angular displacement was indicated on an alternating-current vacuum-tube voltmeter attached to the output of a variable-frequency, narrow-pass-band filter. In essence, the filter performed the function of a Fourier analysis in that both random components and higher harmonics were removed from the signal. In order to measure the phase angle between lift or moment and the angular displacement, the output of the filter was fed into a pulse-shaping circuit designed to convert the sinusoidal signals into pulses corresponding in time to the "crossover" points of the original signal. The pulses were then fed

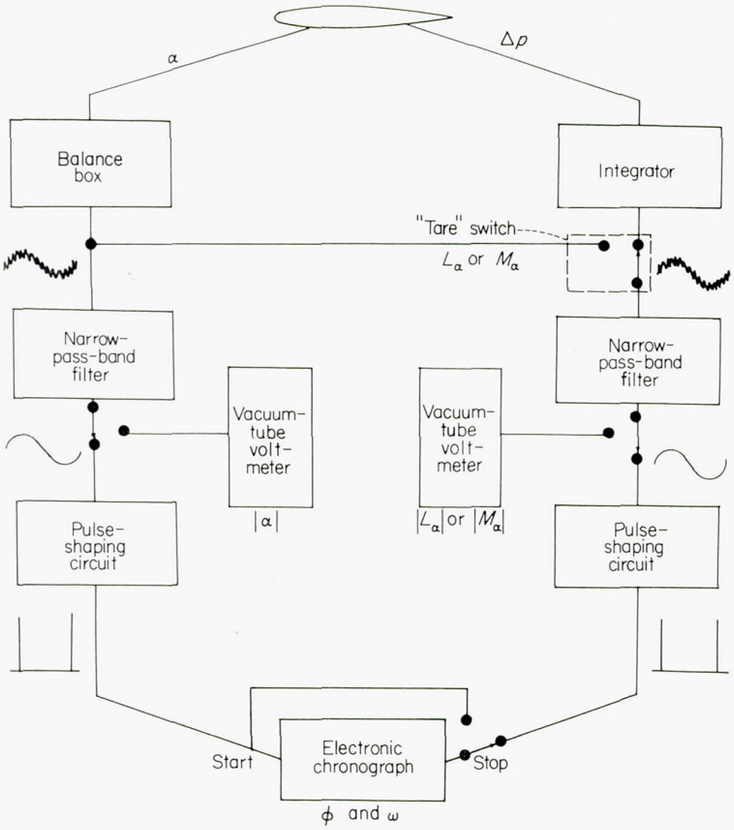

FIGURE 3.—Schematic diagram of instrumentation.

into an electronic chronograph that accurately indicated the time interval between the leading pulse which started the chronograph and the lagging pulse which stopped it. The ratio of this time interval to the period of oscillation, when multiplied by 360°, yields the phase angle in degrees. The period and frequency of oscillation were determined by starting and stopping the chronograph with the angular-displacement signal. In order to minimize the effects of small differences in components between the two circuits, a "tare" switch was provided which fed a single signal (the angular displacement) through both circuits. The resulting phase angle represented the phase shift introduced by the filters and pulse-shaping circuits.

TEST CONDITIONS

The Mach number of the tests was varied from $M=0.35$ to $M=0.7$ and the Reynolds number was held constant at about 5×10^6 by varying the density. The frequency of oscillation was varied from 0 to 60 cycles per second, and the magnitude of angular displacement was about 1.2° except for some lift data at $M=0.71$ which was obtained at an angular displacement of about 2.4°.

DISCUSSION OF RESULTS

The theory and calculation procedure and the experimental technique discussed previously for the determination of the forces acting on a wing oscillating between walls have been applied to a number of specific examples. The investigation has been divided into three parts: (1) A comparison is made of analytical and experimental results obtained for the lift and moment on a pitching wing for several subsonic Mach numbers, (2) theoretical results for the effects of a variation in Mach number at constant tunnel height are given for a pitching wing and also for a wing undergoing vertical translation, and (3) theoretical results for the effects of a variation in the ratio of tunnel height to wing semichord are presented for particular values of Mach number.

COMPARISON OF THEORY AND EXPERIMENT

In figure 4 a comparison is made of analytical and experimental results for a wing oscillating in pitch about its midchord. Figures 4 (a), 4 (b), 4 (c), and 4 (d) apply, respectively, to Mach numbers of 0.35, 0.5, 0.6, and 0.7. The results apply to a ratio of tunnel height to wing semichord H of 7.60.

The plots on the left-hand side of each figure show the magnitudes of the forces and moments as a function of the frequency of oscillation, whereas those on the right-hand side show the corresponding phase angles. The magnitudes are presented as ordinates in the form of ratios $|L_\alpha/L_\alpha'|$ and $|M_\alpha/M_\alpha'|$. In these ratios, the quantities L_α and M_α are, respectively, the lift force and the moment on a wing in a tunnel; L_α' and M_α' are the theoretical lift and the theoretical moment on a wing in free air. The effect of the tunnel walls appears, therefore, as a deviation from unity of the ratios $|L_\alpha/L_\alpha'|$ and $|M_\alpha/M_\alpha'|$ when L_α and M_α are the theoretically derived forces and moments. When L_α and M_α represent the experimental forces and moments, the deviation from unity may not be completely attributed to the effect of tunnel walls because such factors as airfoil thickness and viscosity may cause deviation from the elementary theory. The abscissa in the figures is the ratio of the frequency of the pitching oscillation to a frequency calculated for the resonant condition.

Excellent agreement between theory and experiment is obtained for the phase angles, in most cases, for both the lift and the moment. Quantitatively, however, the agreement between theory and experiment for the magnitudes of the forces is not as good, although very similar trends are demonstrated; in most cases, a systematic difference appears. Some possible sources of the differences between theory and experiment are discussed in the following section.

Examination of figure 4 reveals that the theory predicted the resonant frequency very well. In all cases, the minimum lift and moment were found to lie very close to the analytically indicated resonant frequency. Theoretically, the lift and moment reduce to zero at the resonant condition. Under actual conditions, such as finite tunnel length, transmission of energy through the walls, nonlinearities at higher amplitudes, and turbulence in the flow that gives rise to damping, pure resonance is unobtainable. However, it may be seen by examining figure 4 (d) that the lift and moment were reduced to 20 percent of the values away from resonance.

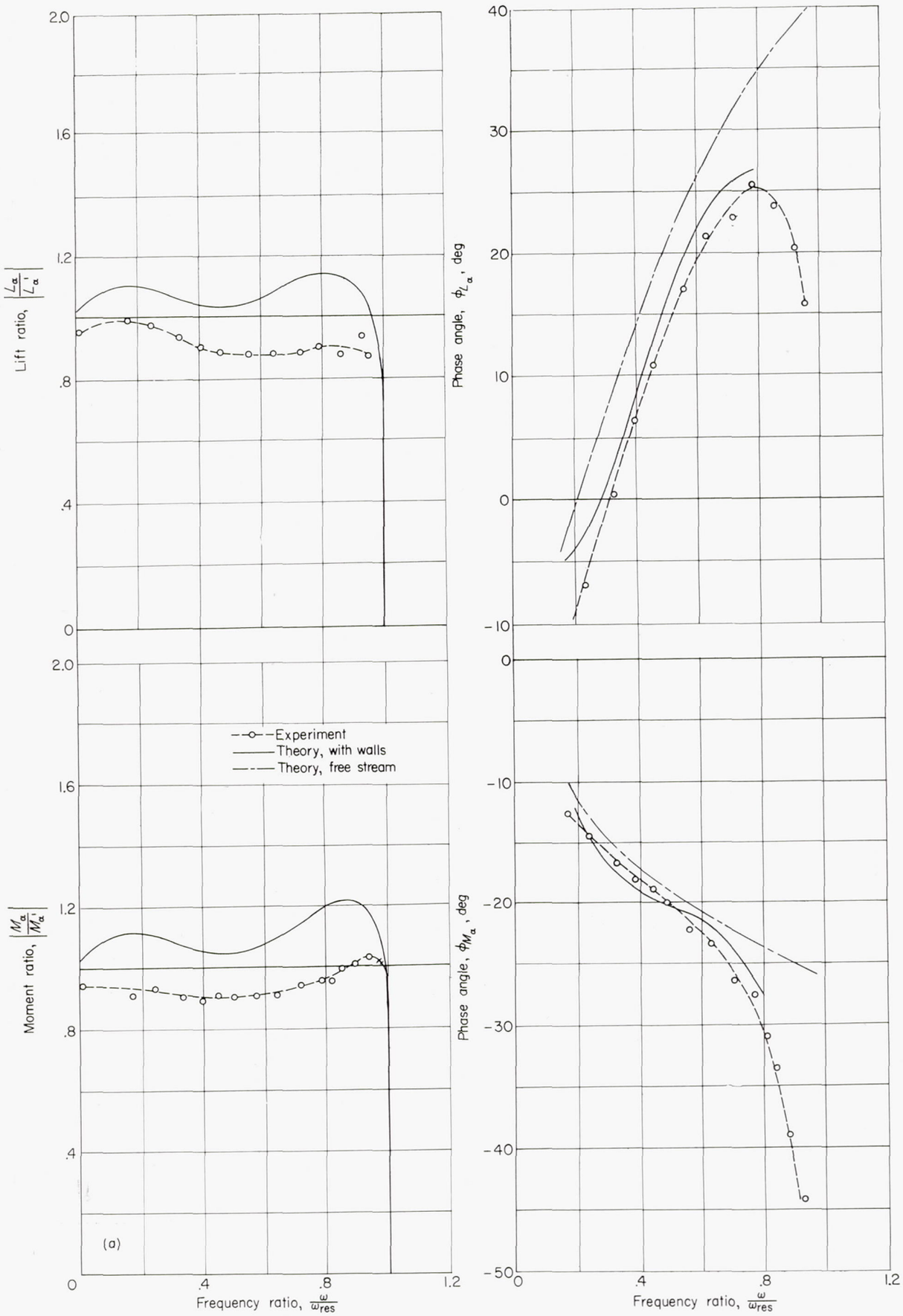

(a) $M=0.35$.

FIGURE 4.—Comparison of theoretical and experimental results for the magnitudes and phase angles of the lift and moment of a pitching wing. Height-semichord ratio $H=7.60$.

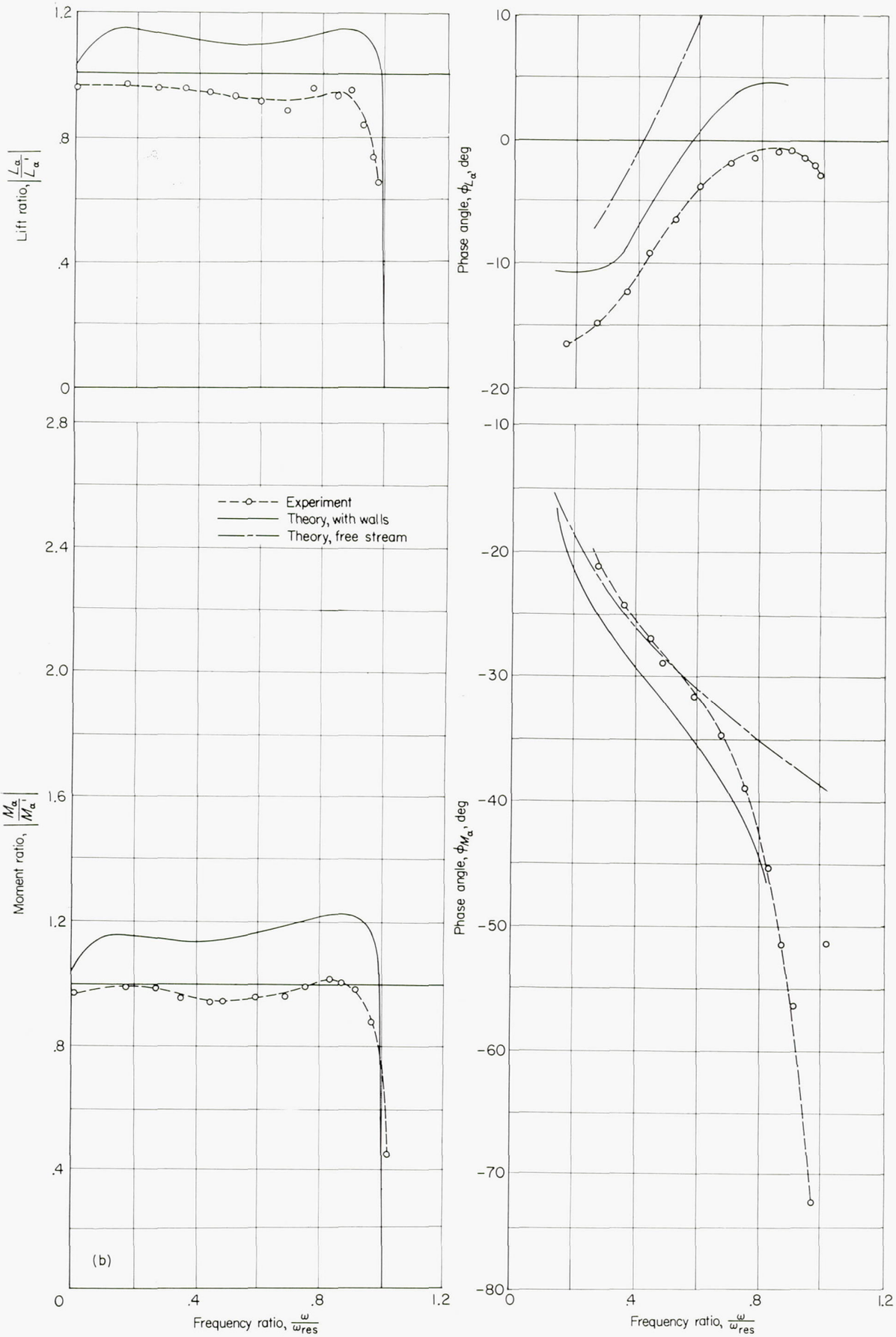

(b) $M=0.5$.

FIGURE 4.—Continued.

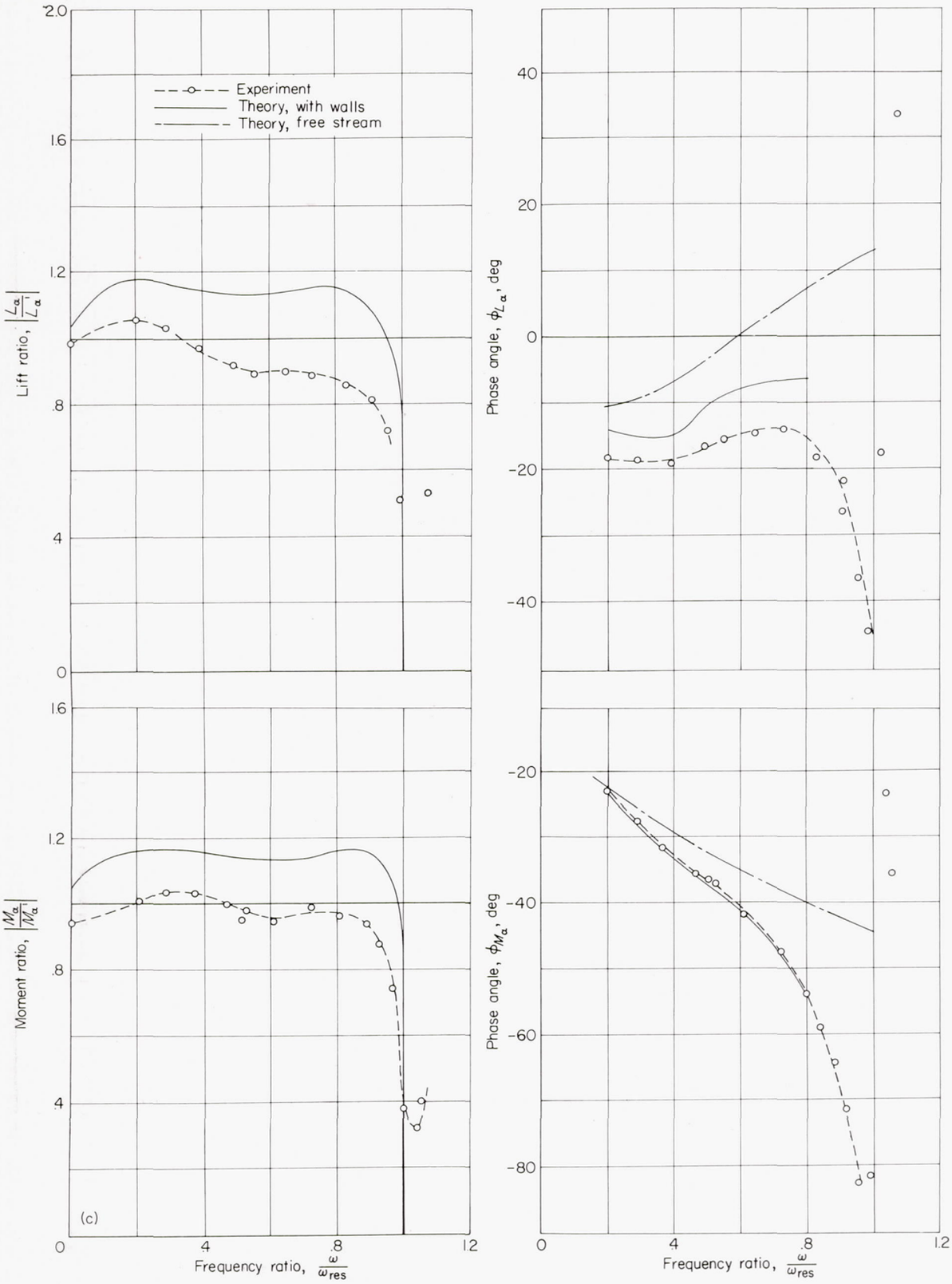

(c) $M=0.6$.

FIGURE 4.—Continued.

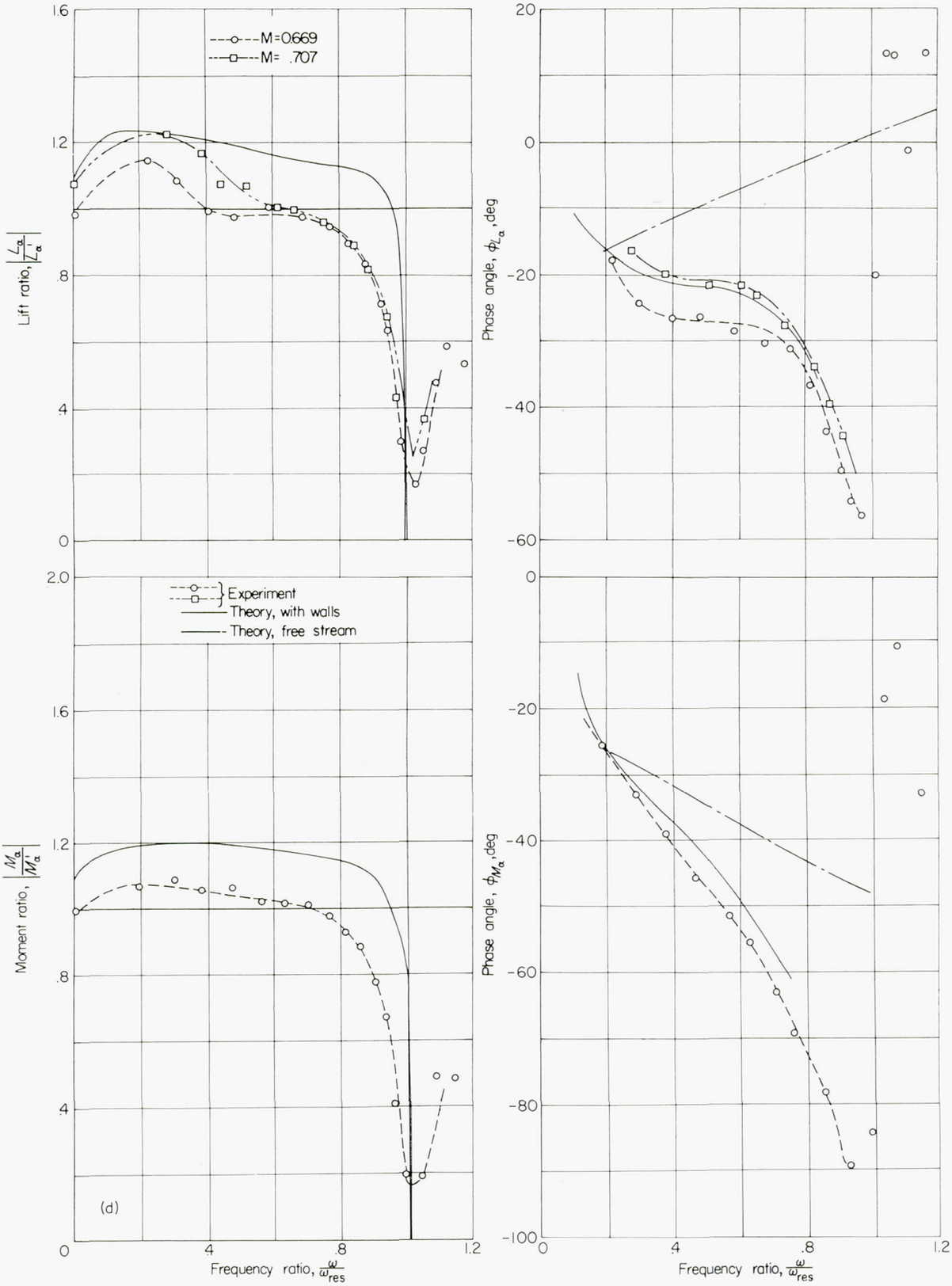

(d) $M=0.7$.

FIGURE 4.—Concluded.

REMARKS ON SOME DIFFERENCES BETWEEN THEORY AND EXPERIMENT

In this section, some limitations and possible reasons for differences between theory and experiment are listed and discussed.

In the comparison between theory and experiment shown in figure 4, an almost constant difference of 10 to 15 percent between the magnitudes is to be noted, whereas the phase angles are in good agreement. Of the several possible reasons for these differences between theory and experiment, perhaps the more important ones are airfoil thickness, Reynolds number, finite tunnel length, transmission of energy through walls, dissipation of the pressure waves due to turbulence, and integration procedures. The effect of all these possibilities is not known for the oscillatory case. In the steady-state case, however, it is known that the effect of increasing thickness is to increase the slope of the lift curve.

In the considerations of the analytical integration, a collocation scheme was used to solve the integral equation. In general, the three collocation points used were found to be satisfactory as pointed out previously.

Twelve pressure cells were used for the experimental integration of the forces. A stepwise integration procedure was employed; that is, the pressure as recorded by the pressure cell was multiplied by an area of the wing over which it is assumed that the cell will give an average pressure. This procedure gives good results except possibly at the leading edge where the pressure variation is very great. Theoretically the pressure approaches infinity at the leading edge $\left(\text{as } \frac{1}{\sqrt{x}}\right)$ and experimentally it is found to be very large. As a matter of fact, if a theoretical distribution of pressure is assumed to be $\cot\frac{\theta}{2}=\sqrt{\frac{1-x}{1+x}}$ as shown in the following sketch and this curve is integrated

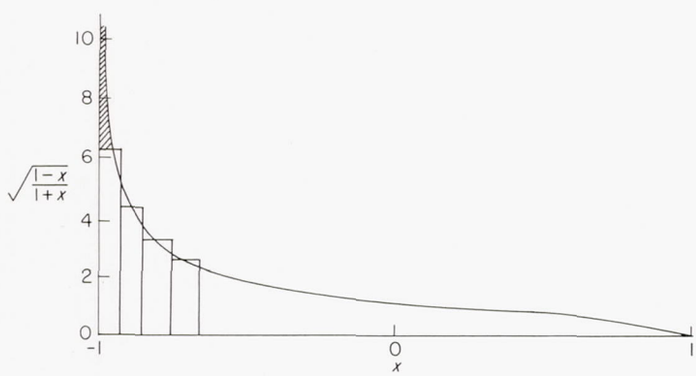

in the same manner as the experimental curve was integrated (that is, by calculating the ordinate at the same value of the abscissa at which the pressure cells were located for the experiment), it is found that the area as determined by the approximate method is 8 percent less than the area as determined by integrating $\cot\frac{\theta}{2}$ in closed form. It is apparent that the neglected area (shaded) can be appreciable. In the actual experiment, in which a fairly thick airfoil was used, the neglected area would probably be smaller but could perhaps contribute to the almost constant difference in magnitudes of lift and moment between the theoretical and experimental results. The effect of this integration difference on the phase angles, which have been shown to be in good agreement, would not be as pronounced.

EFFECT OF A VARIATION IN MACH NUMBER AT CONSTANT TUNNEL HEIGHT

An analytical investigation has been made of the effects of a variation in Mach number at constant tunnel height on the forces on an oscillating wing. Some of the results of the previous section are employed together with results of additional calculations. The magnitudes and associated phase angles of both the lift force and the moment have been determined for a pitching wing and also for a wing undergoing vertical translation. Calculations have been made for a constant value of the height-semichord ratio H of 7.60 and for Mach numbers of 0.3, 0.5, 0.7, and 0.8. Results of the calculations are shown in figures 5 and 6 for the lift and in figures 7 and 8 for the moment.

The magnitudes of the forces and moments are presented, as in the previous section, in the form of ratios: $|L_\alpha/L_\alpha'|$, $|M_\alpha/M_\alpha'|$, $|L_h/L_h'|$, and $|M_h/M_h'|$. The phase angles related to these ratios are presented as a difference between a wing in a tunnel and a wing in free air. The magnitudes and phase angles are plotted against a frequency parameter $\omega\overline{H}/a$, where ω is the circular frequency of oscillation of the wing, $\overline{H}$ is the height of the tunnel, and a is the velocity of sound. At a particular value of the frequency parameter, a progressively larger effect of the walls is indicated as the Mach number increases. At all Mach numbers, the lift is reduced to zero at the resonant frequency. The dip in the curves against frequency ratio, which appears to be characteristic of the low Mach number cases, gradually disappears as the Mach number is increased. As in the case of the magnitude of the lift, the effect of the walls on the phase angle increases as the resonant frequency of the tunnel is approached and also as the Mach number is increased.

The magnitude of the moment about the midchord is shown in figures 7 and 8. The curves have the same shape as the lift-ratio curves and again decrease to zero at the resonant condition. The corresponding phase angles are shown in these figures. Note that in figures 5 to 8 only slight differences appear between results for pitch and those for translation.

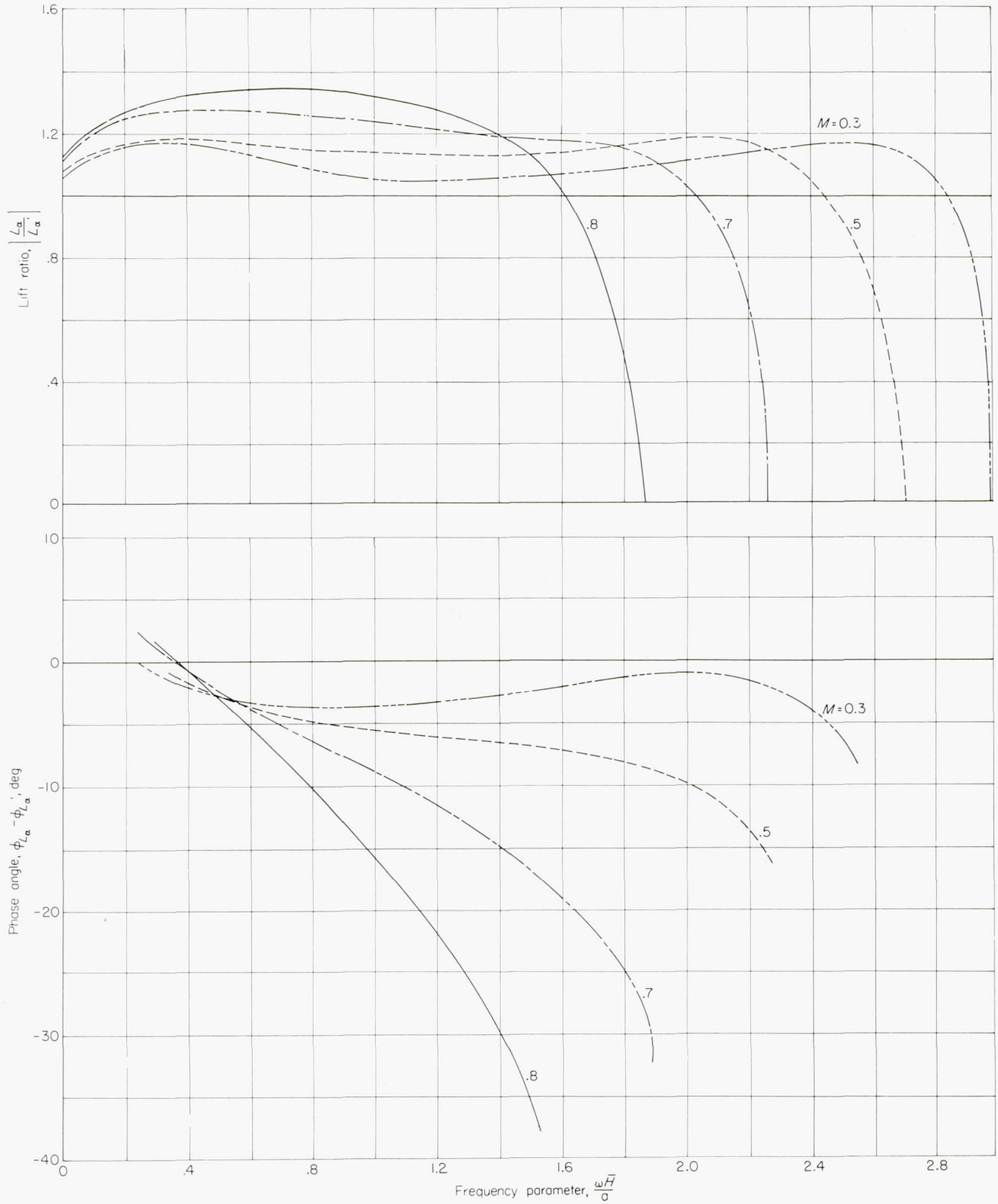

FIGURE 5.—Effect of variation in Mach number at constant height-semichord ratio $H=7.60$ on the magnitude and phase angle of the lift of a pitching wing.

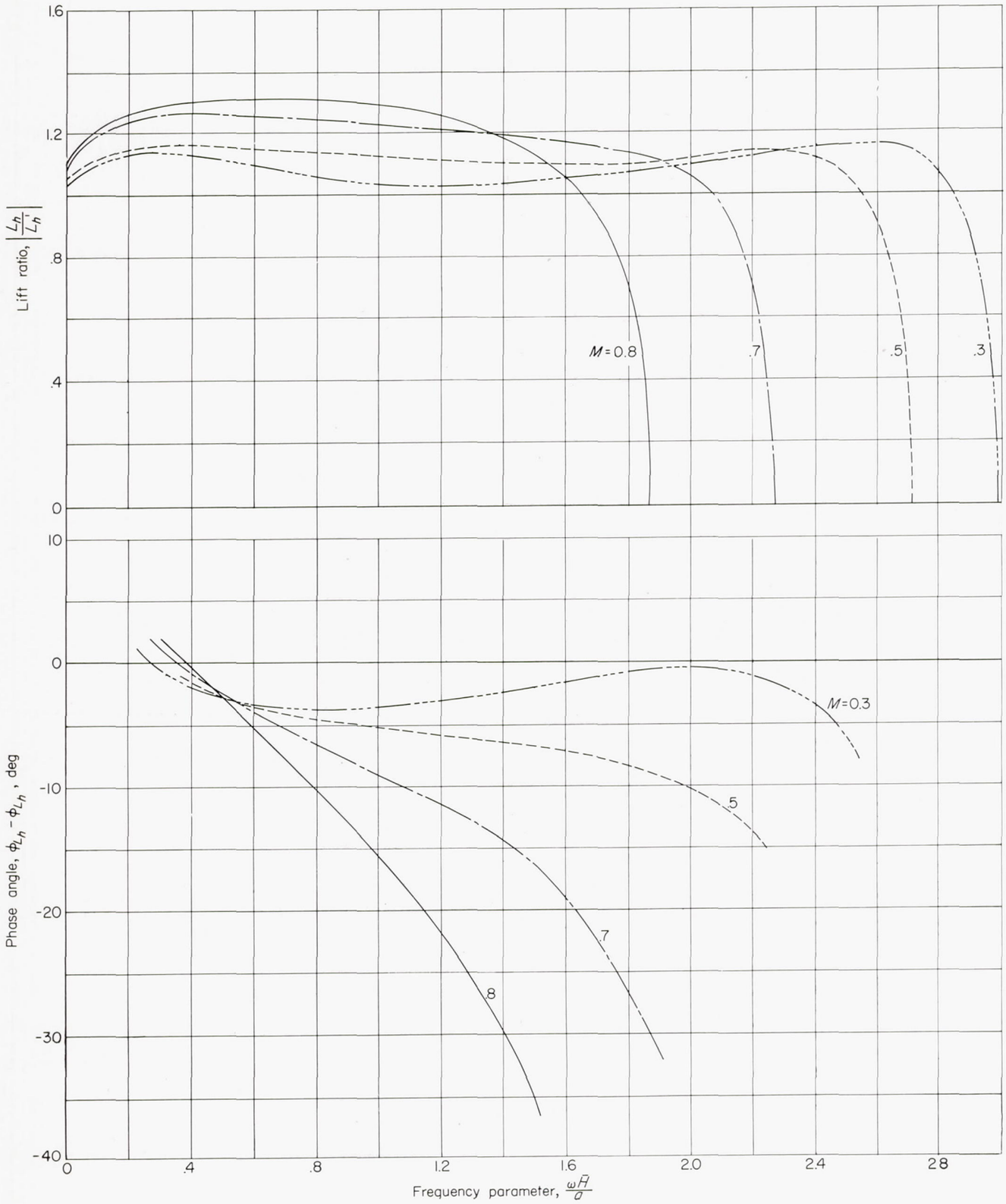

FIGURE 6.—Effect of variation in Mach number at constant height-semichord ratio $H=7.60$ on the magnitude and phase angle of the lift of a translating wing.

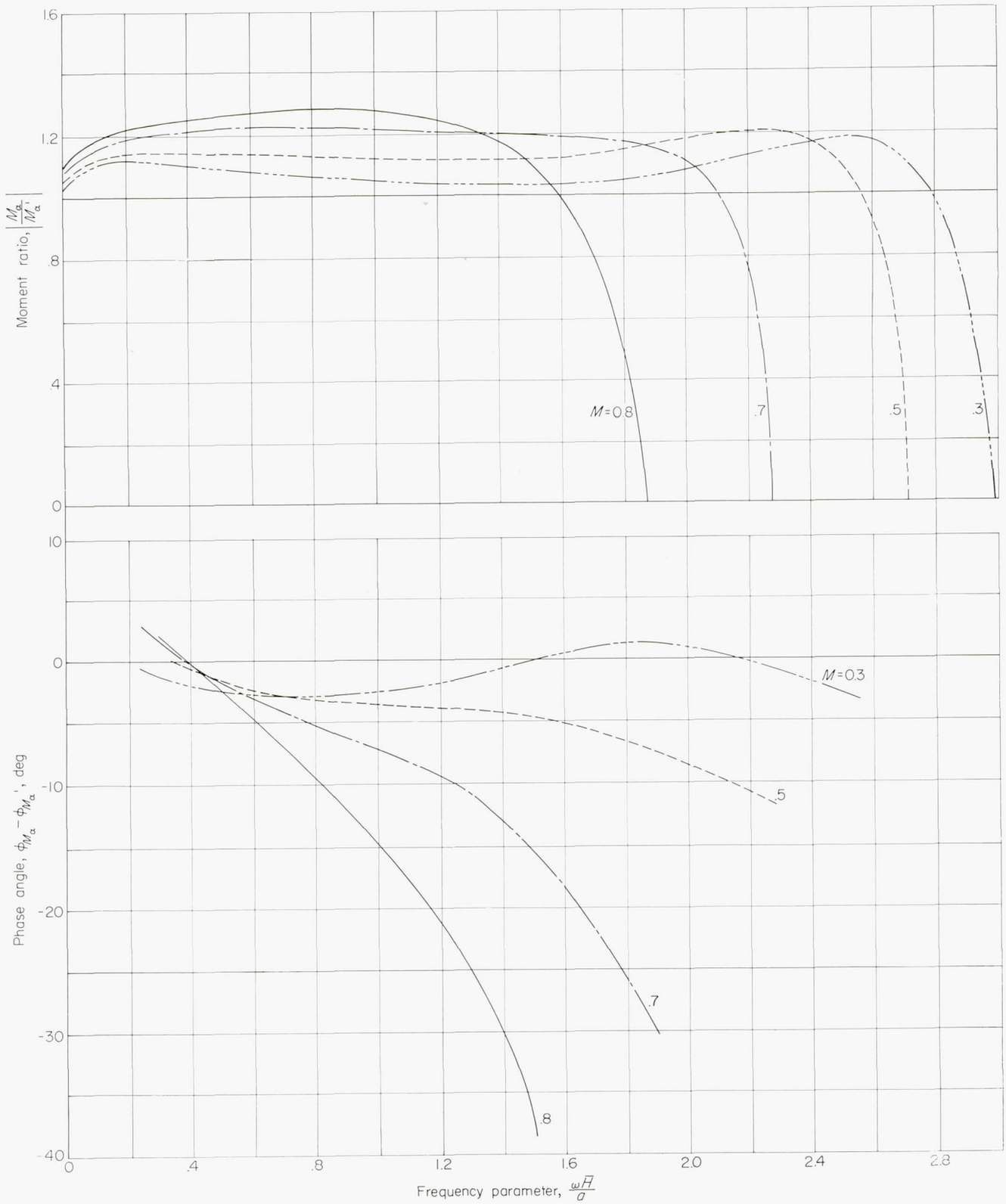

FIGURE 7.—Effect of variation in Mach number at constant height-semichord ratio $H=7.60$ on the magnitude and phase angle of the moment of a pitching wing.

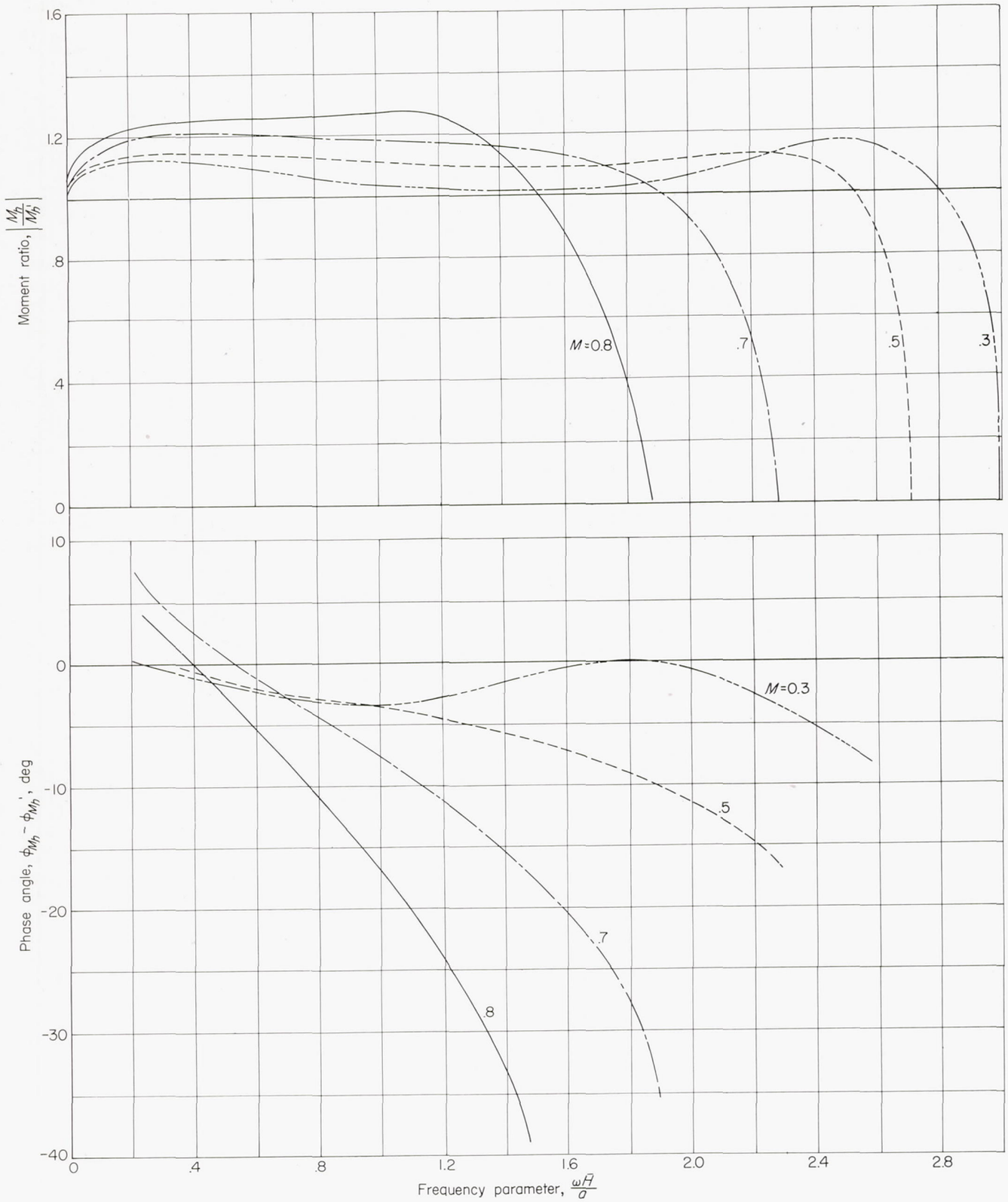

FIGURE 8.—Effect of variation in Mach number at constant height-semichord ratio $H=7.60$ on the magnitude and phase angle of the moment of a translating wing.

EFFECT OF VARIATION IN RATIO OF TUNNEL HEIGHT TO WING SEMICHORD

The effect on the lift-force ratio and on the associated phase angles of varying the ratio of tunnel height to wing semichord is illustrated in figure 9. The results presented in figures 7 and 8 have been based on the consideration of a distribution of pressure doublets over the chord of the airfoil and on satisfying the downwash condition at three chordwise stations. Results for figure 9 have been obtained by the simplified procedure of concentrating the loading in a single doublet at the quarter chord and satisfying the downwash condition at the three-quarter chord. This approach gives fairly good agreement with the results of the more elaborate procedure except near the resonant frequency.

Calculations have again been made for an airfoil oscillating in pitch about its midchord for values of the height-semichord ratio H of 7.60, 16, and 32 at $M=0.3$ and 0.8. In figure 9 (a) the lift ratio $|L_\alpha/L_\alpha'|$ is plotted against the reduced-frequency parameter $k=b\omega/U$. Plots for both Mach numbers are made to the same scale for ease of comparison. It is again apparent that the effect of reducing the Mach number is to reduce the effect of the tunnel walls and to raise the value of the critical frequency at which resonance can occur for a given tunnel. For example, for $H=7.60$, at $M=0.8$, the critical value of k is 0.30, whereas for $M=0.3$, the critical value of k is increased to 1.31. Also, as was to be expected, increasing the height of the tunnel has a marked effect in reducing the influence of the tunnel walls for most of the frequency range. However, the critical frequency is reduced for increased tunnel height so that in the large tunnel the range of k below the fundamental resonance becomes smaller. This reduction in frequency would seem to be a disadvantage of the larger tunnels. However, the second branch of the curve for $H=32$ at $M=0.3$ shows that, for frequencies between the first and second resonant points, the effect of the walls on the magnitude of the lift is no greater than for frequencies below first resonance. Note also that the approach to resonance is quite abrupt; consequently, only a small range of frequencies very close to resonance would be critical and tests could then be conducted between the critical frequencies.

In figure 9 (b) the phase angles, associated with the results of figure 9 (a), for both the wing in a tunnel and for a wing in free air are shown as a function of reduced-frequency parameter k for values of height-semichord ratio H of 7.60, 16, and 32 at $M=0.3$ and 0.8.

At $M=0.3$, the effect of walls on the phase angle is generally very small; at $M=0.8$, the effect is small at low frequencies but increases greatly as the critical value of k is

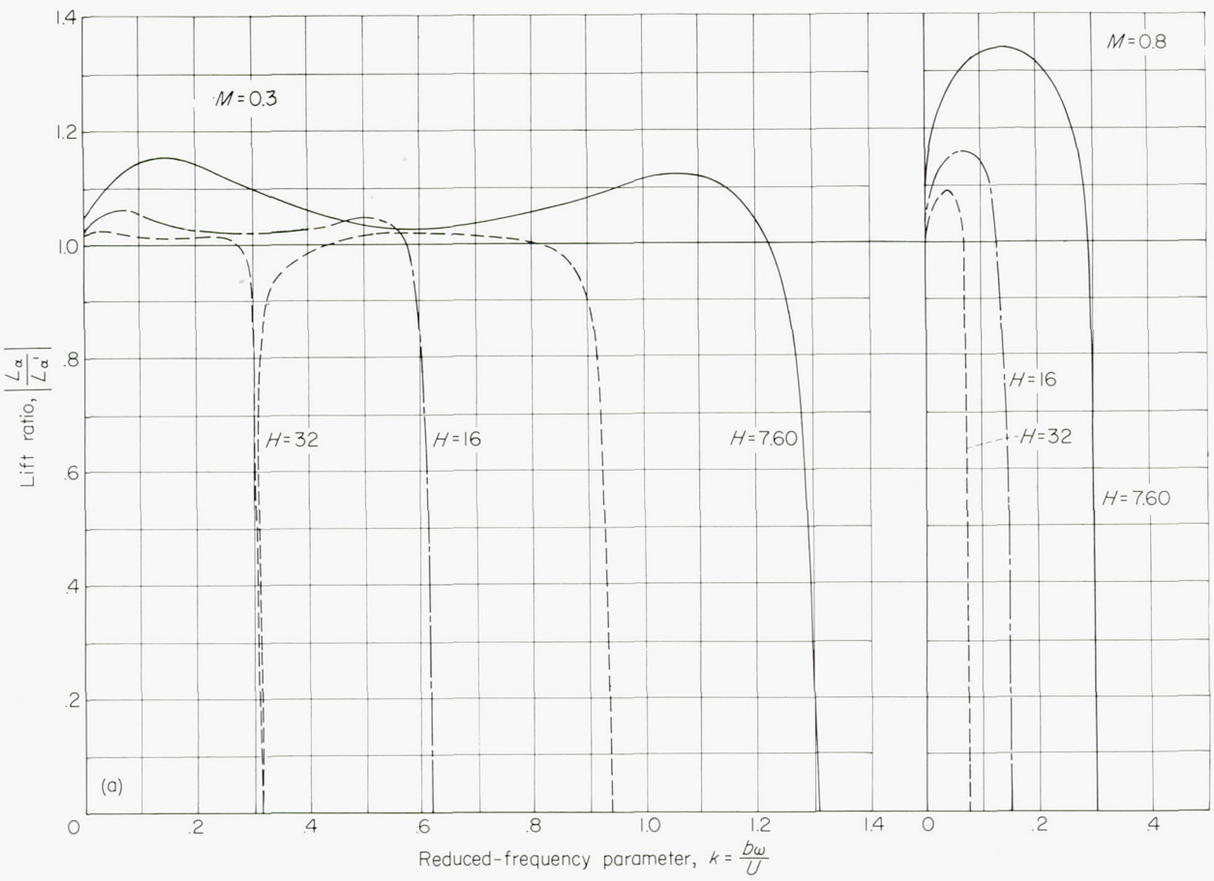

(a) Magnitude of lift.

FIGURE 9.—Effect of a variation in tunnel height on the lift of a pitching wing for $M=0.3$ and $M=0.8$.

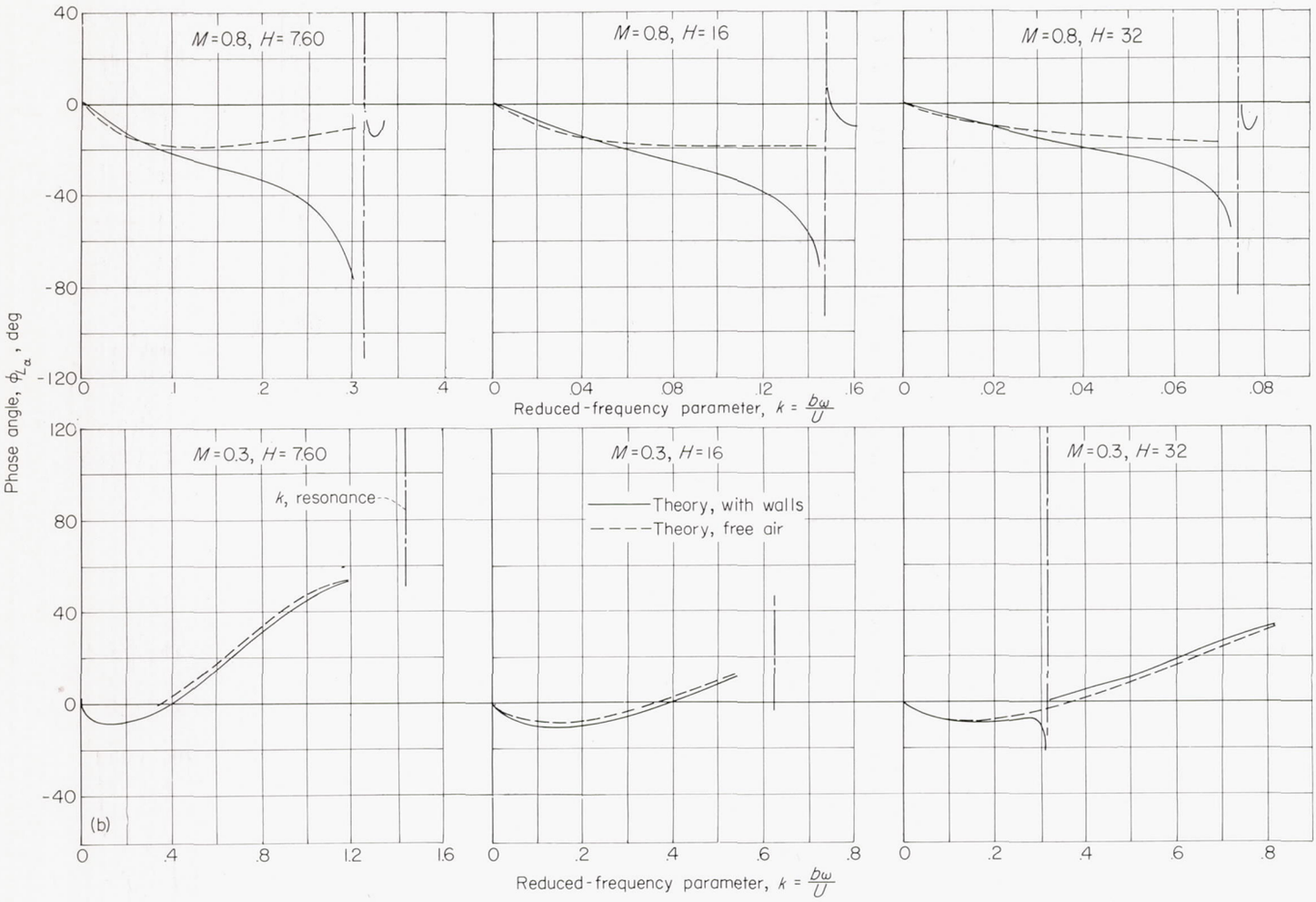

(b) Phase angle of the lift.

FIGURE 9.—Concluded.

approached. As the resonant frequency is approached, results at both Mach numbers show that the phase angle increases in negative value and appears to approach $-90°$. As the resonant condition is exceeded, there is a sudden shift in phase angle. This change is similar to that found for the oscillation of a simple undamped spring-mass system where an abrupt change in phase angle of 180° is found as the resonant frequency is exceeded. Because of the complexity of the kernel, which involves an infinite series of Hankel functions, the phase angle at resonance has not been determined.

In figure 10, the plot from figure 9 (a) for $M=0.3$ and $H=7.60$ is compared with some results of Reissner (ref. 2) for the effect of walls on the lift-force ratio in incompressible flow. This curve for $M=0$ significantly duplicates the rather large wall effect at low values of k which is noted for the $M=0.3$ result. (At low values of k, the curves for the two different Mach numbers are almost coincident probably because of the fact that the slightly lower height semichord ratio $H=6.28$ used by Reissner counteracts the effect of decrease in Mach number.) For values of k greater than 0.5,

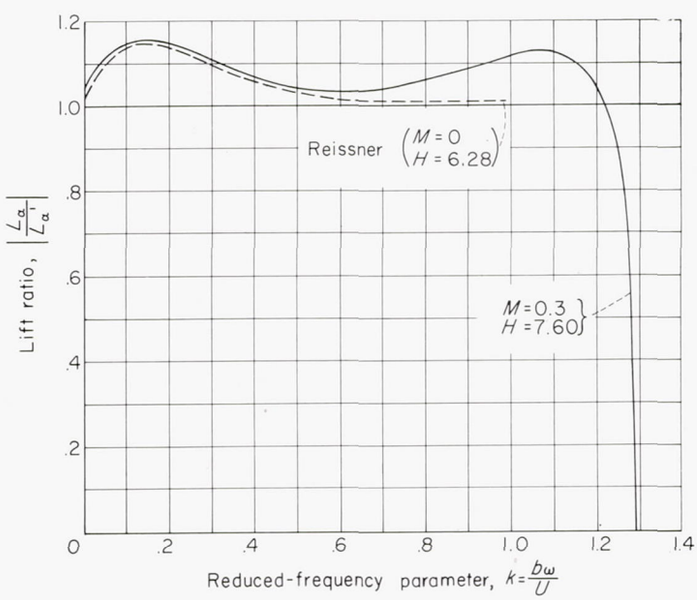

FIGURE 10.—Comparison of lift ratio for $M=0$ and $M=0.3$.

the curves for the two Mach numbers separate; the lift-force ratio at $M=0$ approaches unity and exhibits no effects of resonance because the resonant phenomenon arises only from the effects of compressibility.

CONCLUDING REMARKS

This report has dealt with the problem of an airfoil oscillating between plane walls in subsonic compressible flow. It constitutes a continuation of the work initiated in NACA Report 1150 in that a method of solving the integral equation is presented and some experimental results are compared with theory.

The comparison between theory and experiment for the phase angles between lift force or moment and position is shown to be very good, whereas the comparison between theory and experiment for the magnitudes of the lift and moment is not as good; however, the trends are all accurately predicted. In all cases the resonant frequency was accurately predicted. The cause of the apparent discrepancy between the theoretical and experimental lift and moment may be attributed to several factors such as dissipation of the pressure waves due to turbulence of the air flow and transmission of the energy through the tunnel walls. In addition, the theoretical work was based on the concept of a very thin wing at infinite Reynolds number, whereas the experiments were made with a 10-percent-thick wing at a Reynolds number of approximately 5×10^6. The effect of thickness and Reynolds number have not, as yet, been delineated for the oscillating case.

As would be expected, it is shown theoretically that the larger the tunnel the less the effect of the walls. The critical frequency, however, is also reduced as the tunnel height is increased, but it is shown that tests may be made above the resonant frequency with no larger tunnel-wall effect than is found below the resonance. In addition, the range of influence of the resonant region is greatly reduced so that only a small range of frequencies need be avoided. Wall effects are shown theoretically to be more pronounced as the Mach number is increased and at high Mach numbers are found to be large even at frequencies well removed from resonance.

Langley Aeronautical Laboratory,
National Advisory Committee for Aeronautics,
Langley Field, Va., *January 12, 1955.*

APPENDIX

REDUCTION OF INTEGRAL EQUATION TO THE CASE OF ZERO FREQUENCY

In this appendix, the integral equation for the downwash for a wing oscillating in a compressible medium in the presence of wind-tunnel walls is reduced to the zero-frequency condition.

If equation (1) of the text is written as

$$w(x)=\lim_{\omega\to 0}\frac{b}{\rho U^2}\int_{-1}^{1}L(x_0)[\omega\boldsymbol{K}(M,z)+\omega\boldsymbol{K}(M,z,H)]\,dx_0 \qquad \text{(A1)}$$

and the limit taken as $\omega\to 0$, it will be found that all the terms of $\omega\boldsymbol{K}(M,z)$ and $\omega\boldsymbol{K}(M,z,H)$ vanish except terms involving $H_1^{(2)}$. These terms become infinite; however, as $\omega\to 0$, the asymptotic expansion for very small values of the argument may be used. Therefore,

$$H_1^{(2)}(\mu R_n)=-\frac{2}{\pi i\mu R_n}$$

and

$$\lim_{\omega\to 0}\omega e^{\frac{iz}{\beta^2}}H_1^{(2)}(\mu R_n)i\frac{M(x-x_0)}{R_n}=\frac{-2Ma\beta^2(x-x_0)}{\pi[(x-x_0)^2+\beta^2(nH)^2]}$$

The vertical induced velocity may then be written as

$$w(x)=-\frac{Ma\beta b}{2\pi\rho U^2}\int_{-1}^{1}L(x_0)\left[\frac{1}{x-x_0}+2\sum_{n=1}^{\infty}(-1)^n\frac{x-x_0}{(x-x_0)^2+\beta^2(nH)^2}\right]dx_0 \qquad \text{(A2)}$$

or

$$w(x)=-\frac{Mab}{2\rho U^2H}\int_{-1}^{1}L(x_0)\left[\frac{1}{\frac{\pi}{\beta H}(x-x_0)}+2\sum_{n=1}^{\infty}(-1)^n\frac{\frac{\pi(x-x_0)}{\beta H}}{\frac{\pi^2(x-x_0)^2}{\beta^2H^2}+n^2\pi^2}\right]dx_0 \qquad \text{(A3)}$$

Equation (A3) may be written as

$$w(x)=\frac{-Mab}{2\rho U^2H}\int_{-1}^{1}L(x_0)\left[\operatorname{csch}\frac{\pi(x-x_0)}{\beta H}\right]dx_0 \qquad \text{(A4)}$$

The additional induced velocity due to the presence of tunnel walls for the steady-state case in compressible flow is given by equation (40) of reference 13. Equation (A2) can be reduced to the same form by making the approximation that the airfoil chord is small compared with the tunnel height.

REFERENCES

1. Jones, W. Pritchard: Wind Tunnel Interference Effect on the Values of Experimentally Determined Derivative Coefficients for Oscillating Aerofoils. R. & M. No. 1912, British A.R.C., Aug. 1943.
2. Reissner, E.: Wind Tunnel Corrections for the Two-Dimensional Theory of Oscillating Airfoils. Rep. No. SB–318–S–3, Cornell Aero. Lab., Inc., Apr. 22, 1947.
3. Timman, R.: The Aerodynamic Forces on an Oscillating Aerofoil Between Two Parallel Walls. Appl. Sci. Res. (The Hague), vol. A 3, no. 1, 1951, pp. 31–37.
4. Runyan, Harry L., and Watkins, Charles E.: Considerations on the Effect of Wind-Tunnel Walls on Oscillating Air Forces for Two-Dimensional Subsonic Compressible Flow. NACA Rep. 1150, 1953. (Supersedes NACA TN 2552.)
5. Woolston, Donald S., and Runyan, Harry L.: Some Considerations on the Air Forces on a Wing Oscillating Between Two Walls for Subsonic Compressible Flow. Jour. Aero. Sci., vol. 22, no. 1, Jan. 1955, pp. 41–50.
6. Possio, Camillo: L'Azione aerodinamica sul profilo oscillante in un fluido compressibile a velocita iposonora. L'Aerotecnica, vol. XVIII, fasc. 4, Apr. 1938, pp. 441–458. (Available as British Air Ministry Translation No. 830.)
7. Infeld, L., Smith, V. G., and Chien, W. Z.: On Some Series of Bessel Functions. Jour. Math. and Phys., vol. XXVI, no. 1, Apr. 1947, pp. 22–28.
8. Schwarz, L.: Untersuchung einiger mit den Zylinderfunktionen nullter Ordnung verwandter Funktionen. Luftfahrtforschung, Bd. 20, Lfg. 12, Feb. 8, 1944, pp. 341–372.
9. Frazer, R. A., and Skan, Sylvia W.: Possio's Subsonic Derivative Theory and Its Application to Flexural-Torsional Wing Flutter. Part I—Possio's Derivative Theory for an Infinite Aerofoil Moving at Subsonic Speeds. Part II—Influence of Compressibility on the Flexural-Torsional Flutter of a Tapered Cantilever Wing Moving at Subsonic Speed. R. & M. No. 2553, British A.R.C., 1942.
10. Morse, Phillip M.: Vibration and Sound. Second ed., McGraw-Hill Book Co., Inc., 1948.
11. Patterson, John L.: A Miniature Electrical Pressure Gage Utilizing a Stretched Flat Diaphragm. NACA TN 2659, 1952.
12. Helfer, Arleigh P.: Electrical Pressure Integrator. NACA TN 2607, 1952.
13. Allen, H. Julian, and Vincenti, Walter G.: Wall Interference in a Two-Dimensional-Flow Wind Tunnel, With Consideration of the Effect of Compressibility. NACA Rep. 782, 1944. (Supersedes NACA WR A–63.)

U. S. GOVERNMENT PRINTING OFFICE: 1956